The Stereochemistry and Reactivity of Metal-Schiff Base Complexes. VII. Contribution of Hydrophobic Interligand Interaction to Chiral Recognition of Phenylalaninate and Tryptophanate with (1*R*,2*R*)-*N*,*N*′-Disalicylidene-1,2-cyclohexanediaminecobalt(III) Complex

Yuki FUJII,* Yuzo YOSHIKAWA,† Masato SYOJI, and Homare SHINOHARA
Department of Chemistry, Ibaraki University, Bunkyo, Mito 310
†Department of Chemistry, Faculty of Science, Okayama University, Tsushima, Okayama 700
(Received April 15, 1989)

The stability constants, K_1, of Δ-β_2-diastereomers of mixed ligand cobalt(III) complexes with a chiral quadridentate Schiff base (sal-(*R*,*R*)-chxn), derived from salicylaldehyde and (*R*,*R*)-1,2-cyclohexanediamine, and D- or L-amino acidate (aa^-=gly, ala, val, leu, thr, phe, trp, pro, asp, asn, and glu) were determined spectrophotometrically in water–methanol (2:3 by volume) containing acetate buffer (0.3 mol dm^{-3}) at 22 °C: *trans*-[Co{sal-(*R*,*R*)-chxn}$(H_2O)_2$]$^+$+aa^- $\overset{K_1}{\rightleftharpoons}$ Δ-β_2-[Co{sal-(*R*,*R*)-chxn}(aa)]. The K_1 values range from 5.6×10^6 to 1.2×10^9 mol^{-1} dm^3 and obey a linear free energy relationship except for D-phe, D-trp, D-asp, D-asn, and D-pro. In the cases of D-phe, D-trp, D-asp, and D-asn, their stability constants are 5—30 times as high as those for the corresponding L-aa. Extraordinary stabilization of the D-phe and D-trp complexes is discussed in terms of the interligand stacking of the aromatic rings between the Schiff base ligand and a side chain of amino acidate on the basis of conformational analysis and ^{1}H NMR spectra.

Hydrophobic interligand interaction is one of several interesting subjects in the recent coordination chemistry,[1–3] and much attention has been focused on its contribution to the stereoselectivity of metal chelates[4–7] and the ligand selectivity on metal complexes,[8,9] and on its role in molecular recognition in biological systems.[10,11]

Previously, we reported that mixed ligand Co(III) complexes with a salen-type Schiff base ligand (SB) and L-amino acidate (L-aa), β_2-[Co(SB)(L-aa)], preferentially form Λ_L-diastereomers,[12–18] and that the selectivity is remarkably high when L-aa is *N*-alkyl-L-amino acidates,[15,16,18] L-phenylalaninate (L-phe),[12,13,17] or L-tryptophanate (L-trp).[12,13] For *N*-alkyl-L-amino acidate complexes, their selectivity has been well explained in terms of an interligand steric repulsion between the *N*-alkyl group of amino acidate and the Schiff base ligand in the Λ_L-diastereomers.[16,18] However, in the cases of the L-phe and L-trp complexes, both the side chain of L-amino acidates and the Schiff base ligand are hydrophobic, so that the interligand hydrophobic interactions between them, especially the stacking between aromatic rings rather than steric repulsion, seem to contribute to their selectivity. In order to verify the above possibility and show the effectiveness of hydrophobic interaction for the chiral recognition of amino acids, we investigated here on stability constants of mixed ligand Co(III){sal-(*R*,*R*)-chxn} complexes with eleven L- and D-amino acidates including phe and trp, where sal-(*R*,*R*)-chxn denotes (1*R*,2*R*)-*N*,*N*′-disalicylidene-1,2-cyclohexanediamine. These complexes specifically assume the Δ-β_2-structure,[13,16,18] so that those with D-form amino acidates belong to stabler diastereomers in this system,[19] except for prolinate.[15] In addition, conformational analyses and ^{1}H NMR measurements were conducted for L- and D-phe and L- and D-ala complexes to support the contribution of the hydrophobic interaction.

Experimental

Preparation of Complexes. ***trans*-[Co{sal-(*R*,*R*)-chxn}$(H_2O)_2$]$ClO_4\cdot CH_3OH$:** [Co{sal-(*R*,*R*)-chxn}][20] (2.5 g, 6.6×10^{-3} mol) in 250 cm^3 of methanol was stirred for 2 h under air oxidation conditions to form a dark brown solution. $HClO_4$ (2%, 100 cm^3) was added to it, and the solution was concentrated to a small volume (about 40 cm^3) at room temperature. The dark brown crystals, thus formed, were recrystallized from methanol.

Δ-β_2-[Co{sal-(*R*,*R*)-chxn}(aa)] (aa=L-ala, D-ala, L-phe, D-phe, L-trp, and D-trp): Since the preparative method is almost the same for all the complexes, only a representative procedure for the D-phe complex is described here. D-Phenylalanine (0.22 g, 1.33×10^{-3} mol) was added to a solution of [Co{sal-(*R*,*R*)-chxn}] (0.5 g, 1.32×10^{-3} mol in 30 cm^3 of methanol), the solution was stirred for 3 h under air oxidation conditions. After filtration, the filtrate was evaporated almost to dryness at room temperature. The resulting green powder was dissolved in acetone (20 cm^3) and then water (3 cm^3) was added. The solution was concentrated slowly to a small volume to give a green powder. It was washed with water and air dried.

The yield, elemental analysis, and characterization data are summarized in Tables 1 and 2.

Solution Equilibria. The acid dissociation constants, K_{a_1} and K_{a_2}, of *trans*-[Co{sal-(*R*,*R*)-chxn}$(H_2O)_2$]ClO_4 were determined by spectrophotometric titration at 340 nm in water and in a mixed solvent of water and methanol (2:3 by volume) at 22 °C:

$$[Co(SB)(H_2O)_2]^+ \overset{K_{a_1}}{\rightleftharpoons} [Co(SB)(OH)(H_2O)] + H^+, \quad (a)$$

$$[Co(SB)(OH)(H_2O)]^+ \overset{K_{a_2}}{\rightleftharpoons} [Co(SB)(OH)_2]^- + H^+. \quad (b)$$

The spectral variation for the reaction (a) showed isosbestic

points at 300, 350, 390, and 420 nm, and that for (b) those at 310, 360, 400, 430 nm. The estimated K_{a_1} and K_{a_2} values are listed in Table 3.

The formation constant, K_{ac}, of *trans*-[Co{sal-(*R*,*R*)-chxn}-(CH_3COO)(H_2O)] and the stability constants, K_1, of Δ-β_2-[Co{sal-(*R*,*R*)-chxn}(aa)] were determined spectrophotometrically in water–methanol (2:3 by volume) at pH 5.75 and 22 °C. The K_{ac} and K_1 values are summarized in Tables 3 and 4, respectively.

The pH in water–methanol was measured by the use of a glass electrode (Horiba #6326-06c) and the activity of proton was calculated by $p_a(H)$=pH−0.22.[21] All the chemicals used here were reagent grade and used without further purification.

Conformational Analysis. Empirical force field (strain energy minimization) calculations were carried out in a manner similar to that described in the preceding paper.[22] The electronic charges of the lone-paired electrons on the coordinated oxygen atoms were assumed to be equally −0.2. The initial coordinates were completed due to the coordination calculation options in the MM2 program on the basis of those of the Co(III)–salen complex.

Measurements. The electronic absorption and CD spectra were measured with a Hitachi 320 spectrometer at 22 °C and with a JASCO J-20 spectropolarimeter at room temperature, respectively. The optical rotations at 435 nm were measured with a JASCO DIP-140 polarimeter at 22 °C. The ^1H NMR spectra were recorded with a JEOL GSX-400 (400 MHz)

Table 1. Characterization Data

Complex[a]	Yield/%	Elemental analysis (%)[b]			$[M]^{22}_{435}$ in methanol
		C	H	N	
trans-[Co(SB)(H_2O)$_2$]ClO_4·CH_3OH	90	46.08 (46.12)	5.20 (5.16)	5.17 (5.12)	−12400
Δ-β_2-[Co(SB)(D-phe)]·2.5H_2O	75	59.10 (59.18)	6.16 (5.99)	7.00 (7.14)	+30000
Δ-β_2-[Co(SB)(L-phe)]·H_2O	67	62.05 (62.03)	5.78 (5.74)	7.32 (7.48)	+31600
Δ-β_2-[Co(SB)(D-trp)]·H_2O	72	62.10 (62.00)	5.46 (5.54)	9.33 (9.33)	+30000
Δ-β_2-[Co(SB)(L-trp)]·H_2O	51	61.95 (62.00)	5.43 (5.54)	9.55 (9.33)	+29800
Δ-β_2-[Co(SB)(D-ala)]·4.5H_2O	67	50.48 (50.37)	6.26 (6.43)	7.74 (7.66)	+36300
Δ-β_2-[Co(SB)(L-ala)]·0.5H_2O	49	57.97 (57.99)	5.85 (5.71)	8.90 (8.82)	+39100

a) SB=sal-(*R*,*R*)-chxn. b) The values in parentheses are calculated ones.

Table 2. Electronic Absorption (AB) and CD Spectral Data of Δ-β_2-[Co{sal-(*R*,*R*)-chxn}(aa)] in Methanol[a]

aa in complex	AB $\{\tilde{\nu}$ (log $\varepsilon)\}$	CD $\{\tilde{\nu}$ ($\Delta\varepsilon)\}$	aa in complex	AB $\{\tilde{\nu}$ (log $\varepsilon)\}$	CD $\{\tilde{\nu}$ ($\Delta\varepsilon)\}$
D-phe	17.09(2.52)	16.72(−8.89)	L-phe	17.01(2.57)	16.34(−9.22)
	21.74(2.68)[b]	19.84(−1.35)		21.50(2.73)[b]	19.84(−1.22)
	26.32(3.73)	23.26(+8.96)		26.18(3.78)	23.31(+9.83)
	31.75(3.60)[b]	24.81(+8.88)		31.75(3.67)[b]	24.51(+7.10)
		27.70(+13.37)			27.86(+14.00)
D-trp	17.24(2.53)	16.72(−9.24)	L-trp	17.01(2.57)	16.42(−9.00)
	21.05(2.52)[b]	19.62(−1.62)		21.28(2.69)[b]	19.84(−1.19)
	26.32(3.75)	23.26(+9.09)		26.32(3.73)	23.26(+9.60)
	31.75(3.64)[b]	25.00(+8.42)		31.75(3.68)[b]	24.51(+9.41)
		27.78(+13.23)			27.86(+13.26)
D-ala	17.09(2.63)	16.58(−10.73)	L-ala	17.09(2.63)	16.58(−10.21)
	21.28(2.70)[b]	19.62(−1.11)		21.28(2.70)[b]	19.69(−2.13)
	26.32(3.83)	23.26(+11.21)		26.25(3.83)	23.36(+11.07)
	31.25(3.67)[b]	24.75(+11.35)		31.45(3.69)[b]	24.75(+11.30)
		27.78(+16.70)			27.70(+16.82)

a) Wavenumbers are given in 10^3 cm^{-1}. b) Shoulder.

Table 3. Thermodynamic Data for *trans*-[Co{sal-(*R*,*R*)-chxn}(H_2O)$_2$]$^+$ at 22 °C

Solvent	K_{a_1}	K_{a_2}	K_{ac}[c]
H_2O–MeOH[a]	(3.55±0.05)×10^{-8}	b)	3.99±0.02
H_2O	(1.80±0.05)×10^{-7}	(6.0±0.1)×10^{-13}	

a) 2:3 by volume. b) A side reaction occurred. c) Formation constant of monoacetatocomplex.

spectrometer at an ambient probe temperature.

Results and Discussion

Determination of Stability Constants. As an acetate buffer (0.3 mol dm^{-3} CH_3COOH+0.3 mol dm^{-3} CH_3COONa) was used in the measurements of the stability constants of Δ-β_2-[Co{sal-(*R*,*R*)-chxn}(aa)], first of all, the complexation between *trans*-[Co{sal-(*R*,*R*)-chxn}$(H_2O)_2$]$^+$ and acetate ion was investigated. Figure 1 shows the absorption spectra of mixtures of *trans*-[Co{sal-(*R*,*R*)-chxn}$(H_2O)_2$]ClO_4 and acetate buffer at various concentrations, and Fig. 2(a) represents the variation of the absorbance at 560 nm of the solutions. The observed spectra exhibit isosbestic points at 448 and 497 nm, but no spectral change was observed in the presence of acetic acid alone. Thus, the following equilibrium is assumed to be established:

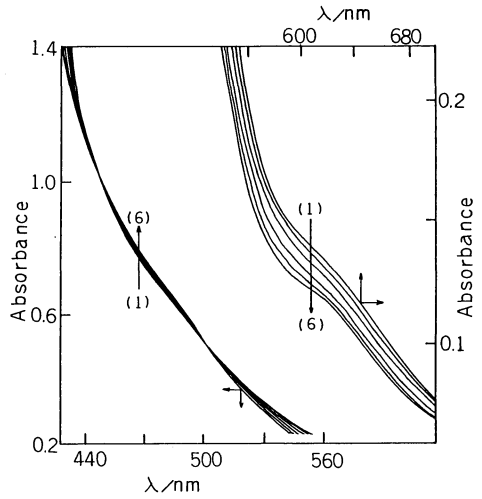

Fig. 1. Spectral changes of *trans*-[Co{sal-(*R*,*R*)-chxn}$(H_2O)_2$]$^+$ with acetate buffer (pH=5.75) in water-methanol (2:3 in volume). Complex: 1.0×10^{-3} mol dm^{-3}; Acetate buffer: (1)=0, (2)=4.2×10^{-2}, (3)=8.0×10^{-2}, (4)=2.0×10^{-1}, (5)=4.0×10^{-1}, and (6)=6.0×10^{-1} mol dm^{-3}.

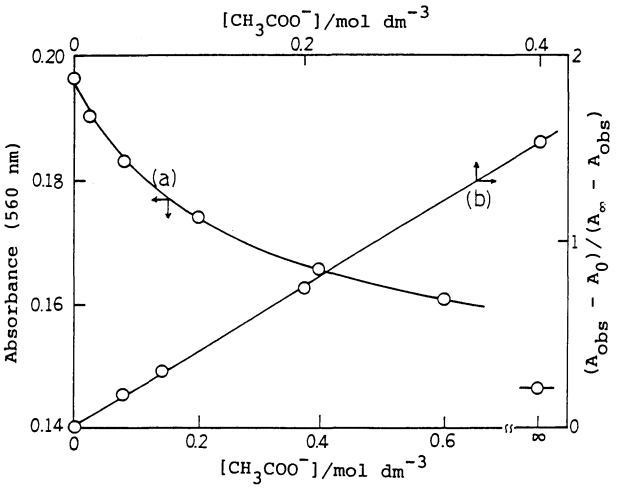

Fig. 2. Variation of absorbance at 560 nm of *trans*-[Co{sal-(*R*,*R*)-chxn}$(H_2O)_2$]$^+$ in the presence of acetate buffer (pH=5.75) in water-methanol (2:3 by volume) and plot of $(A_{obs}-A_0)/(A_\infty-A_{obs})$ vs. $[CH_3COO^-]$.

trans-[Co{sal-(*R*,*R*)-chxn}$(H_2O)_2$]$^+$ + CH_3COO^-

$$\overset{K_{ac}}{\rightleftharpoons} \textit{trans}\text{-[Co\{sal-(}R,R\text{)-chxn\}}(CH_3COO)(H_2O)]. \quad (1)$$

The equilibrium constant, K_{ac}, was estimated to be 3.99 from the slope of the plot of $(A_{obs}-A_0)/(A_\infty-A_{obs})$ vs. $[CH_3COO^-]$ (Fig. 2(b)) by the use of the method of Marzilli et al.,[23] where A_0, A_∞, and A_{obs} denote the absorbances at 560 nm of [Co(SB)$(H_2O)_2$]$^+$, [Co(SB)$(CH_3COO)(H_2O)$], and their mixture, respectively. The obtained K_{ac} value indicates that two species of complexes, [Co(SB)$(H_2O)_2$]$^+$ and [Co(SB)$(CH_3COO)(H_2O)$], exist in about 1:1 molar ratio in the presence of 0.3 mol dm^{-3} acetate buffer. In the present study, the deprotonated species [Co(SB)$(OH)(H_2O)$] was neglected, because its concentration was estimated to be negligibly small at pH 5.75 from the K_{a_1} value of the diaqua complex.

Figure 3 shows the representative spectra of the mixtures of *trans*-[Co{sal-(*R*,*R*)-chxn}$(H_2O)_2$]ClO_4 and amino acid in the presence of acetate buffer. The spectra exhibit isosbestic points at about 537 and 680 nm for all the amino acids investigated, and the spectra in the presence of an excess of amino acids correspond to those of β_2-[Co(salchxn)(aa)].[13,15] Hence, the following equilibria can be written:

trans-[Co{sal-(*R*,*R*)-chxn}$(H_2O)_2$]$^+$ + aa^-

$$\overset{K_1}{\rightleftharpoons} \Delta\text{-}\beta_2\text{-[Co\{sal-(}R,R\text{)-chxn\}(aa)]}, \quad (2)$$

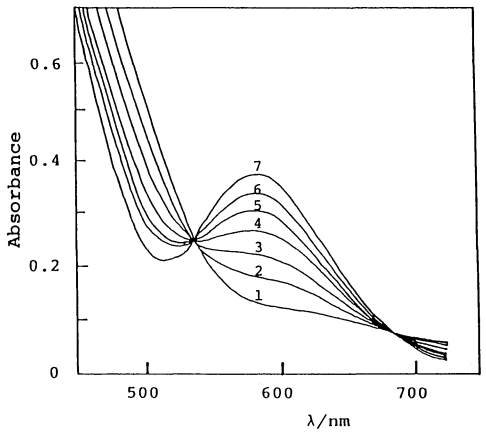

Fig. 3. Spectral changes of *trans*-[Co{sal-(*R*,*R*)-chxn}$(H_2O)_2$]$^+$ with D-phenylalanine in the presence of acetate buffer (0.3 mol dm^{-3}) in water-methanol (2:3 by volume). Complex: 1.0×10^{-3} mol dm^{-3}; D-phe: 1=0, 2=2.0×10^{-4}, 3=4.0×10^{-4}, 4=6.0×10^{-4}, 5=8.0×10^{-4}, 6=1.0×10^{-3}, and 7=20×10^{-3} mol dm^{-3}.

$$\textit{trans}\text{-[Co\{sal-(}R,R\text{)-chxn\}(CH}_3\text{COO)(H}_2\text{O)] + aa}^- \underset{}{\overset{K_2}{\rightleftharpoons}} \Delta\text{-}\beta_2\text{-[Co\{sal-(}R,R\text{)-chxn\}(aa)] + CH}_3\text{COO}^-, \quad (3)$$

where K_1 and K_2 represent the stability constants of Eqs. 2 and 3, K_1=[Co(SB)(aa)]/[Co(SB)$(H_2O)_2$][aa] and K_2=[Co(SB)(aa)]/[Co(SB)$(CH_3COO)(H_2O)$][aa]. The K_1 and K_2 are related to the absorbance of solutions by

$$\begin{aligned}(A_0 - A_{obs})/(A_{obs} - A_\infty) &= [Co(SB)(aa)]/[Co]_{free} \\ &= K_1[AA]/\alpha_H(1 + K_{ac}[CH_3COO^-]) \\ &= K_2K_{ac}[AA]/\alpha_H(1 + K_{ac}[CH_3COO^-]), \end{aligned} \quad (4)$$

where, A_0, A_∞, and A_{obs} denote the absorbances (580 nm) of $[Co]_{free}$, [Co(SB)(aa)], and their mixture, respectively. $[Co]_{free}$, [AA], and α_H represent the sum of concentrations of $[Co(SB)(H_2O)_2]^+$ and [Co(SB)$(CH_3$-COO)(H_2O)], the total concentration of free amino acid, and the α_H value of amino acid, respectively. As is shown in Fig. 4, the plot of $(A_0-A_{obs})/(A_{obs}-A_\infty)$ vs. [AA] gives a straight line through the origin for all the amino acids studied. Thus, the stability constants, K_1, can be estimated from the slpoe, and the obtained K_1 values are summarized in Table 4.

Figure 5 shows the effect of acetate buffer on the K_{obs} values, where $K_{obs}=K_1/\alpha_H(1+K_{ac}[CH_3COO^-])$. Since the plot of K_{obs} vs. $(1+K_{ac}[CH_3COO^-])^{-1}$ exhibits a linear relation through the origin, this result clearly indicates that the stability constants, K_1, are not influenced by acetate buffer.

Comparison of Stability Constants. It has been known that [Co{sal-(*R*,*R*)-*chxn*}(aa)] preferentially assumes the Δ-β_2 structure regardless of the configuration (L or D) of coordinated amino acidates.[13,16,19] This selectivity for the Δ-configuration is due to the steric effect of (R,R)-chxn group. Also in the cases of the phe, trp, and ala complexes prepared here, they show a strong CD peak with minus sign at about 600 nm regardless of the chirality of the coordinated amino acidates (Table 2), and the CD spectra correspond to the Δ-β_2 structure. In addition, their ^{1}H NMR spectra

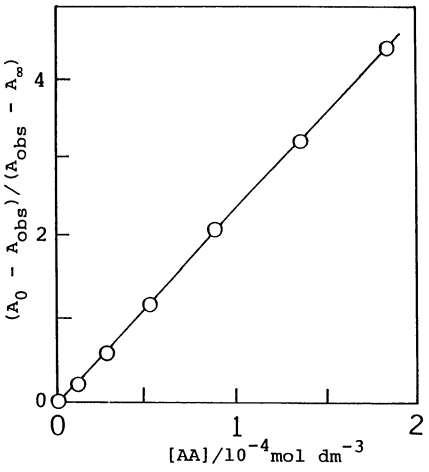

Fig. 4. Plot of $(A_0-A_{obs})/(A_{obs}-A_\infty)$ vs. [AA] for the formation of Δ-β_2-[Co{sal-(*R*,*R*)-chxn}(D-phe)] in the presence of acetate buffer (0.3 mol dm^{-3}) in water-methanol (2:3 by volume).

Table 4. Stability Constants, K_1, of Δ-β_2-[Co{sal-(*R*,*R*)-chxn}(aa)] in Water-Methanol (2:3 by Volume) Containing Acetate Buffer (0.3 mol dm^{-3}) at 22 °C

Amino acid			$K_{obs}/10^{3b)}$	$K_1/10^7$	K_1^D/K_1^L	$\Delta(\Delta G)$/kJ mol^{-1}
aa$^-$	pK_a[a)]	Optical form				
gly	3.13, 9.23		2.9 ±0.1	2.6 ±0.1		
ala	3.28, 9.41	L	1.2 ±0.1	1.6 ±0.2	1.25	0.55
		D	1.5 ±0.1	2.0 ±0.2		
val	3.26, 9.26	L	1.2 ±0.1	1.2 ±0.1	1.25	0.55
		D	1.5 ±0.1	1.5 ±0.1		
leu	3.31, 9.28	L	1.8 ±0.1	1.8 ±0.1	1.22	0.50
		D	2.2 ±0.1	2.2 ±0.1		
phe	3.13, 8.77	L	4.0 ±0.1	1.3 ±0.05	7.25	4.90
		D	29 ±1	9.4 ±0.3		
trp	3.17, 9.06	L	6.4 ±0.1	3.9 ±0.1	29.7	8.37
		D	190±20	115 ±15		
pro	2.80, 10.00	L	1.4 ±0.2	7.4 ±1	0.14	−4.80
		D	0.2 ±0.02	1.1 ±0.1		
thr	3.10, 8.70	L	2.1 ±0.1	0.56±0.03	3.86	3.33
		D	8.1 ±0.1	2.2 ±0.03		
asp	2.77, 4.40, 9.70	L	1.6 ±0.1	4.2 ±0.3	5.25	4.10
		D	8.4 ±0.1	22 ±0.3		
asn	2.89, 8.56	L	2.9 ±0.1	0.56±0.02	6.55	4.65
		D	19 ±1	3.7 ±0.2		
glu	2.96, 4.85, 9.63	L	1.3 ±0.1	2.9 ±0.3	1.54	1.07
		D	2.0 ±0.1	4.5 ±0.3		

a) pH titration in water-methanol (2:3 by volume) containing $NaClO_4$ (0.3 mol dm^{-3}). b) pH=5.75.

show that each complex consists of only one species, indicating that the complexes assume the Δ-β_2 structure exclusively. It has also known that Co(III) complexes with salen-type Schiff bases are liable to substitution and isomerization.[24,25] Thus, the difference in stability constant between the L- and D-amino acidate complexes corresponds to the free energy difference between the Δ_L-β_2- and Δ_D-β_2-diastereomers and reflects the difference in interligand interaction between them.

Table 4 indicates that the energy difference between L- and D-isomers comes up to 4—8 kJ mol^{-1} in the cases of phe, trp, pro, asp, and asn. In order to solve the question whether the differences arise mainly from the stabilization or destabilization of one of the two diastereomers, the plot of log K_1 vs. pK_a of amino acids was examined. The results is shown in Fig. 6. Generally, this kind of plot shows a linear relationship with a slope of 0.5—2 depending upon the nature of metal–ligand bonds, when interligand interactions are negligibly small.[26] In the present case, we set up an area which is surrounded by lines with slopes of 0.5 and 2.0 through the point of alaninate as shown in Fig. 6, and considered that amino acidates which deviate largely from this area are involved in a strong interligand interaction. In the case of prolinate, it has been assumed that its selectivity comes mainly from steric repulsion, i.e., destabilization of one of the two diastereomers.[15] In fact, as is seen in Fig. 6, D-pro deviates largely below the area, although L-pro fits to the area, which supports that the stereospecificity of the Co{sal-(*R*,*R*)-chxn} system for L-pro is based on the destabilization of D-pro complex by steric repulsion. In the cases of phe, trp, asp, and asn, the D-forms deviate largely above the area, and the L-forms fit to the area. Hence, the stereospecificity for the D-isomers of these amino acidates can be assigned safely to extraordinary stabilization of the stable diastereomer, Δ_D-β_2-form. As a factor of interligand interactions, which is responsible for the large stabilization of the D-phe and D-trp complexes, the hydrophobic interaction between aromatic rings is the most probable.[3,8,11] On the other hand, in the cases of the D-asp and D-asn complexes, the intramolecular hydrogen bonding between amino group and carboxylate or carboamide group may contribute to their stabilization.[27]

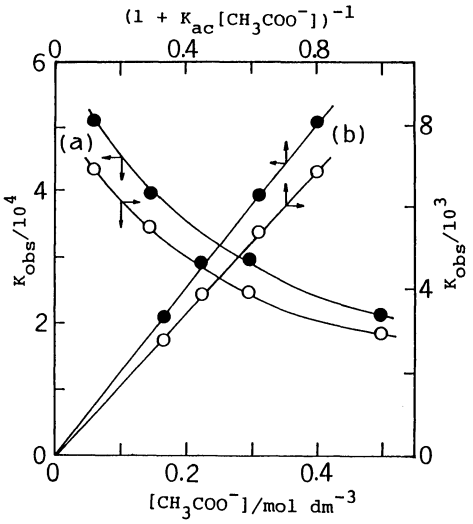

Fig. 5. Effect of acetate buffer on the observed stability constants, K_{obs}, of Δ-β_2-[Co{sal-(*R*,*R*)-chxn}-(phe)] in water–methanol (2:3 by volume). ●: D-phe, ○: L-phe.

Conformational Analysis. In order to get further information about the hydrophobic interaction mentioned above, a conformational analysis was carried out for the D- and L-ala and the D- and L-phe

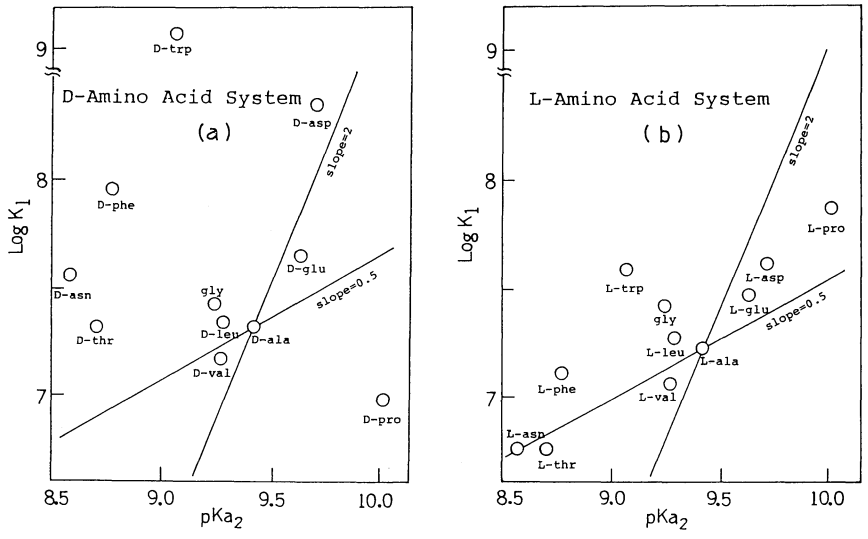

Fig. 6. Plots of stability constants of Δ-β_2-[Co{sal-(*R*,*R*)-chxn}(aa)] vs. pK_a values of amino acids.

Table 5. Results of Energy Minimization Calculation for β-[Co{sal-(*R*,*R*)-chxn}(aa)]

Structure of complex	Coordinated amino acidate	Notation of conformer	Dihedral angle/°	Energy/kJ mol^{-1}					
				Bonding	Bending	Nonbonded	Torsion	Charge	Total
Δ-β$_2$ (*mer*)	D-phe	*g*	+172.3	8.28	44.00	50.76	−6.28	139.01	235.75
		h	−57.6	8.28	45.28	47.14	−5.60	138.71	233.81
		t	+55.6	8.33	42.93	46.97	−5.74	138.81	231.31
	L-phe	*g*	−174.9	8.26	41.63	50.65	2.66	138.92	242.12
		h	+62.4	8.13	44.47	43.67	2.10	139.30	237.69
		t	−52.3	7.76	44.42	45.55	2.50	139.22	239.45
	D-ala			7.43	42.10	41.88	20.00	138.93	250.34
	L-ala			8.14	41.71	41.69	19.34	140.44	251.32
Δ-β$_1$ (*fac*)	D-phe	*t*	+56.8	9.59	47.66	43.79	−3.25	151.26	249.05
	L-phe	*h*	+53.1	8.46	47.42	38.31	11.09	151.78	257.06

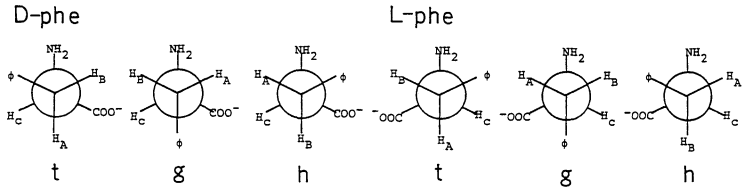

Fig. 7. Conformation of amino acidates and notation thereof.

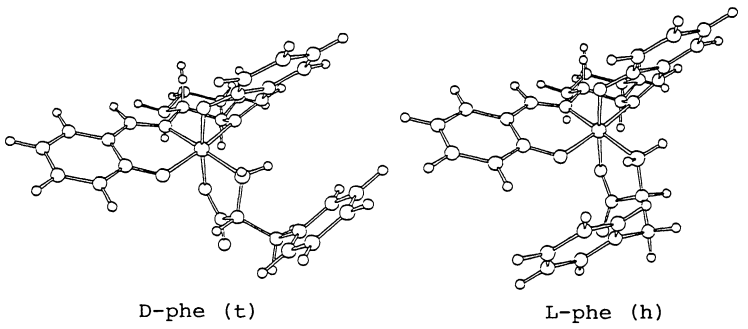

Fig. 8. Ortep drawings of the *t* and *h* conformers for D-phe and L-phe complexes, respectively.

complexes. The results are summarized in Table 5, where *t*, *g*, and *h* represent rotamers around -C(α)H-C(β)H$_2$- carbon atoms of the coordinated phenylalaninate, which are distinguished by the dihedral angle between the amino and phenyl groups. In this study, angles are taken as anticlockwise. The conformers, *t*, *g*, and *h*, are shown in Fig. 7.

Table 5 suggests that the stablest conformer is *t* for D-phe and *h* for L-phe. Their structures are shown in Fig. 8. The total energy difference between the *t* (D-phe) and *h* (L-phe) conformers is estimated to be 6.38 kJ mol^{-1}, which is in good agreement with the observed one, 4.90 kJ mol^{-1}, at 22 °C in solution. Also in the case of the ala complexes, the estimated value (0.98 kJ mol^{-1} stabler in D-ala) is close to the observed one (0.55 kJ mol^{-1}). In addition, the stablest conformer for the D-phe complex belongs to the *t* from, and this form coincides with observed ones in X-ray studies for similar Schiff base complexes.[7,14,28] Therefore, the present results of our conformational analysis seem to agree well with the observed ones. However, the main energy difference between the L- and D-phe complexes is based on the torsional one, whereas that between the L- and D-ala complexes comes from the bonding one. Further, there was seen no distinguishable difference in Co–O and Co–N bond lengths among the six conformers of L- and D-phe complexes (Co–O$_5$=1.903±0.003 Å, Co–O$_6$=1.904±0.001 Å, Co–O$_7$=1.914±0.002 Å, Co–N$_2$=1.943±0.003 Å, Co–N$_3$=1.914±0.001 Å, and Co–N$_4$=1.903±0.002 Å for the six conformers). Thus, in order to evaluate the hydrophobic interligand interaction in the phe complexes, the nonbonded interactions between the phenyl group of phe and the aromatic ring of the Schiff base ligand

Table 6. Nonbonded Energy between the Phenyl Group of Phe and the Aromatic Group of the Schiff Base (Part A in Fig. 9) of Δ-β_2-Diastereomers

Amino acidate	Conformer	Energy/kJ mol^{-1}	Amino acidate	Conformer	Energy/kJ mol^{-1}
D-phe	*g*	−0.29	L-phe	*g*	−0.31
	h	−3.53		*h*	−0.99
	t	−2.96		*t*	−2.08

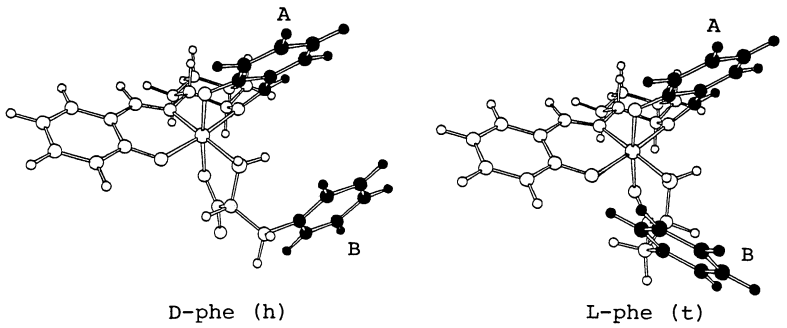

Fig. 9. Non-bonded interaction between aromatic part (A) of Schiff base and phenyl group (B) in D-phe (*h*) and L-phe (*t*) complexes.

(part A in Fig. 9) were calculated. The results in Table 6 indicate that 1) the interaction stabilizes every system, 2) it is more effective in D-phe than in L-phe, and that 3) the increasing order of the stabilization of the conformers is $g \ll t < h$ for D-phe and $g < h < t$ for L-phe. Although these orders do not completely coincide with the orders of total energy, they agree well with the results of the ^{1}H NMR study to be mentioned later, which indicates that the stacking between the phenyl group of phe and one of the aromatic rings of the Schiff base is responsible for the extraordinary stabilization of the D-phe complex in solution.

We also calculated the energy for the Δ-β_1(*fac*) isomers of L- and D-phe (Table 5). Clearly, the β_1(*fac*) isomers are much more unstable than the β_2(*mer*) isomers (ca. 17.6 kJ mol^{-1}), the energy difference corresponding to the isomeric ratio (*fac*:*mer*) of 1:1200. Since the energy difference comes mainly from the charge, the observed high regioselectivity (100%) for the β_2 (*mer*) isomer is ascribed to the fact that the electrostatic repulsion among the three coordinated oxygen atoms is much smaller in β_2(*mer*) than in β_1-(*fac*).

^{1}H NMR Spectra. The ^{1}H NMR data are listed in Table 7 and the representative spectra are shown in Fig. 10.

In the case of the D-phe complex, one of the two H–C=N protons, one of the two 1-protons on the salicylidene groups, some CH and CH_2 protons on chxn, and the 5 and 5′ protons on the phenyl group of D-phe shift to higher field as compared with those of the L- and D-ala and L-phe complexes. A similar higher field shift is observed for the D-trp complex. The

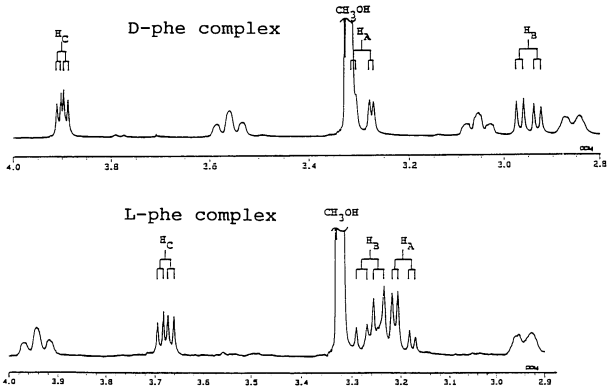

Fig. 10. ^{1}H NMR spectra of Δ-β_2-[Co{sal-(*R*,*R*)-chxn}-(phe)] in CD_3OD+D_2O (4:1 by volume).

higher field shift for the D-phe complex is comparable to the estimated value for the *h*-conformer from the Johnson–Bovey diagram on the basis of the conformational analysis data. Thus, these higher field shifts are due to the ring current effect of the phenyl (indolyl) group of D-phe (D-trp) and one of the salicylidene groups of the Schiff base ligand, which indicate that the phenyl (indolyl) group faces one of the salicylidene groups (A in Fig. 9) by assuming the *h* conformation. In fact, the ^{1}H NMR analysis (Table 8)[29] indicates that the D-phe and D-trp complexes have a high *h* conformer distribution (50—60%). The amount of conformers increases in the order of $g < t < h$, and this order coincides with that of the aromatic ring-ring interaction (stabilization) for the D-phe complex (Table 6). Therefore, it can be concluded that the D-

Table 7. ^{1}H NMR Spectral Data for Δ-β_2-[Co{sal-(*R*,*R*)-chxn}(aa)][a]

Complex	H-C=N	chxn					Amino acidate										
							-CH-	-CH$_2$-									
		1,1'[a]	2,2'[b]	3,3'[b]	4,4'[a]	-CH-[b]	Hc	H$_A$	H$_B$	5,5'[a]	6,6'[b]	7[b]	5[f]	6[a]	7[b]	8[b]	9[a]
D-ala	8.20	7.49	6.79	7.32	7.19	4.00	3.80[c]	1.32 (-CH$_3$)[a]									
	7.74	7.46	6.67	7.16	6.93	3.28											
L-ala	8.21	7.52	6.79	7.33	7.19	3.96	3.48[c]	1.52 (-CH$_3$)[a]									
	7.77	7.48	6.68	7.17	6.91	3.29											
D-phe	8.15	7.44	6.82	7.32	7.17	3.56	3.90[d]	3.30[d]	2.95[d]	7.05[a]	7.40[b]	7.47[b]	6.95	7.12	7.00	7.23	7.55
	6.99	7.35	6.67	7.17	6.87	3.06											
L-phe	8.19	7.49	6.74	7.32	7.06	3.93	3.67[d]	3.19[d]	3.27[d]	(7.35, 7.36)[e]			7.15	7.41	7.06	7.15	7.78
	7.76	7.45	6.67	7.10	6.86	3.20											
D-trp	8.13	7.44	6.76	7.31	7.17	3.14	3.85[d]	3.47[d]	3.18[d]								
	6.52	7.44	6.67	7.12	6.83	2.97											
L-trp	8.17	7.45	6.66	7.29	7.02	3.94	3.68[d]	3.34[d]	4.47[d]								
	7.70	7.36	6.65	7.02	6.81	3.21											

chxn: 1.93, 2.16, 1.40, 1.98, 2.52, 1.76, 1.50 / 1.87, 1.42, 1.31, 1.18 / 1.96, 2.50, 1.76, 1.48 / 1.76, 2.80, 1.58, 1.87, 2.91, 1.88

a) Doublet. b) Triplet. c) Quartet. d) Two doublets. e) AB_2C pattern. f) Singlet. g) Solvent=CD_3OD+D_2O (4:1 by volume).

Table 8. Population of Conformers for Δ-β_2-[Co{sal-(*R*,*R*)-chxn}(aa)][a]

aa	J_{AC}[b]	J_{BC}[b]	Conformers/%[29]		
			h	*t*	*g*
D-phe	3.300	5.866	60	32	8
L-phe	4.580	8.612	23	57	20
D-trp	1.836	6.968	53	42	5
L-trp	4.400	9.164	20	62	18

a) Solvent: CD_3OD(80%)+D_2O(20%). b) Coupling constant of -CH(α)-CH$_2$(β)- protons of amino acidate.

phe and D-trp complexes favor the *h* conformation for the cordinated amino acidates due to the stabilization through the aromatic ring–ring interaction as a main factor.

In the cases of the L-phe and L-trp complexes, a higher field shift is observed for the 3 and 4 protons of the salicylidene groups (Table 7), and the higher field shift for the L-phe complex is comparable to the estimated shift for the *g*-conformer from the Johnson–Bovey diagram. Hence, these facts suggest that the phenyl and indolyl groups face one of the salicylidene groups (A in Fig. 9) by assuming the *t* conformation. In fact, the ^{1}H NMR analysis shows a high *t* conformer distribution (ca. 60%) for the L-phe and L-trp complexes. The order in amount of conformers is $g<h<t$, and this order coincides with that of the aromatic ring–ring interaction for the L-phe complex (Table 6). Hence, the L-phe and L-trp complexes are also stabilized by the aromatic ring–ring interaction. Since the stabilization is larger in D-phe and D-trp than in L-phe and L-trp, the stability constants for the D-phe and D-trp complexes deviate largely upward from the free energy relationship (Fig. 6). It should also be due to the aromatic ring–ring interaction that the stability constants for the L-phe and L-trp complexes are somewhat higher than those expected from the free energy relationship.

For the aromatic ring–ring interaction, the shortest interatomic distance between the benzene rings, the distance between their centers, and their inter-facing angles in the *h* and *t* conformers of the D-phe complex are calculated as follows on the basis of the results of the conformational analysis: 4.14 Å, 6.00 Å, and 18.4° for the *h* conformer, and 4.42 Å, 5.61 Å, and 23.9° for the *t* conformer. In the case of the *t* conformer of the L-phe complex, they are 4.24 Å, 7.26 Å, and 12.0°. These data suggest that the benzene rings are not completely parallel to each other and that their centers do not coincide with each other. The shortest interatomic distances between the benzene rings are 4.1—4.4 Å in the present systems, which are longer than that for [Ch(histamine)(L-trp)] (3.45 Å),[3] suggesting that the aromatic ring–ring interaction is effective in a long range in the Co(III)–Schiff base system.

References

1) E. Frieden, *J. Chem. Educ.*, **52**, 754 (1975).

2) H. Okawa and S. Kida, *Kagaku No Ryoiki*, **37**, 276 (1983).

3) O. Yamauchi and A. Odani, *Nippon Kagaku Kaishi*, **1988**, 369.

4) M. Nakamura, H. Okawa, T. Inazu, and S. Kida, *Bull. Chem. Soc. Jpn.*, **55**, 2400 (1982); M. Nakamura, H. Okawa, T. Ito, M. Kato, and S. Kida, *ibid.*, **60**, 539 (1987).

5) K. Kashiwabara, I. Kinoshita, T. Ito, and J. Fujita, *Bull. Chem. Soc. Jpn.*, **54**, 725 (1981); M. Atoh, I. Kinoshita, K. Kashiwabara, and J. Fujita, *ibid.*, **55**, 3179 (1982).

6) A. Tatehata, *Inorg. Chem.*, **21**, 2496 (1982).

7) Y. Fujii, H. Shinohara, M. Mikuriya, S. Kida, and Y. Konishi, *Bull. Chem. Soc. Jpn.*, **61**, 3511 (1988).

8) H. Sigel, R. M. Balakrishnan, and U. K. Haring, *J. Am. Chem. Soc.*, **107**, 5137 (1985); H. Sigel, R. Tribolet, and K. H. Scheller, *Inorg. Chim. Acta*, **100**, 151 (1985).

9) O. Yamauchi and A. Odani, *Inorg. Chim. Acta*, **100**, 165 (1985).

10) R. M. Milburn, M. G. Basak, R. Tribolet, and H. Sigel, *J. Am. Chem. Soc.*, **107**, 3315 (1985); R. Tribolet, R. M. Balakrishnan, and H. Sigel, *J. Chem. Soc., Dalton Trans.*, **1985**, 2291.

11) O. Yamauchi and A. Odani, *J. Am. Chem. Soc.*, **107**, 5938 (1985); A. Odani, S. Deguchi, and O. Yamauchi, *Inorg. Chem.*, **25**, 62 (1986); O. Yamauchi, A. Odani, R. Shimata, and Y. Kosaka, *ibid.*, **25**, 3337 (1986); O. Yamauchi, A. Odani, R. Shimata, and S. Ishiguro, *Recl. Trav. Chim. Pays-Bas*, **106**, 196 (1987).

12) Y. Fujii, T. Isago, M. Sano, N. Yanagibashi, S. Hirasawa, and S. Takahashi, *Bull. Chem. Soc. Jpn.*, **49**, 3509 (1976).

13) Y. Fujii, M. Sano, and Y. Nakano, *Bull. Chem. Soc. Jpn.*, **50**, 2609 (1977).

14) K. Kushi, R. Tamura, M. Kuramoto, T. Yoshizawa, H. Yoneda, and Y. Fujii, *J. Chem. Soc., Chem. Commun.*, **1978**, 266.

15) Y. Fujii, K. Shiono, K. Ezuka, and T. Isago, *Bull. Chem. Soc. Jpn.*, **53**, 3537 (1980).

16) Y. Fujii, M. Matsufuru, A. Saito, and S. Tsuchiya, *Bull. Chem. Soc. Jpn.*, **54**, 2029 (1981).

17) Y. Fujii, Y. Kuwana, S. Takahashi, K. Shimizu, and K. Hiroi, *Bull. Chem. Soc. Jpn.*, **55**, 2598 (1982).

18) Y. Kushi, T. Tada, Y. Fujii, and H. Yoneda, *Bull. Chem. Soc. Jpn.*, **55**, 1834 (1982).

19) In previous papers,[13,16] we used sal-(*S,S*)-chxn ligand. In the present study, as we used sal-(*R,R*)-chxn, the relation between the absolute configuration of complex and the chirality of coordinated amino acidates is reverse to that in the sal-(*S,S*)-chxn system.

20) H. Aoi, M. Ishimori, S. Yoshikawa, and T. Tsuruta, *J. Organomet. Chem.*, **85**, 241 (1975).

21) H. Yoshimura, H. Matsushita, and T. Morimoto, "Theory and Measurements of pH," Maruzen, Tokyo (1968), p. 415.

22) C. Fukuhara, S. Matsuda, K. Katsura, M. Mori, K. Matsumoto, S. Ooi, and Y. Yoshikawa, *Inorg. Chim. Acta*, **142**, 203 (1988).

23) L. G. Marzilli, P. A. Marzilli, and J. Helpern, *J. Am. Chem. Soc.*, **93**, 1374 (1971).

24) G. Costa, *Coord. Chem. Rev.*, **8**, 63 (1972).

25) Y. Fujii, T. Kobayashi, M. Matsufuru, and S. Takahashi, *Bull. Chem. Soc. Jpn.*, **56**, 3608 (1983).

26) M. Tanaka, "Chemistry of Solvent Extraction," Kyoritu Syuppan, Tokyo (1977), p. 36.

27) Y. Kojima and M. Shibata, *Inorg. Chem.*, **12**, 1009 (1973).

28) K. Okamoto, K. Matsutani, and Y. Fujii, *Bull. Chem. Soc. Jpn.*, **58**, 3486 (1985).

29) The population was calculated by the use of J_{AC} and J_{BC} of ABX pattern for $-CH(\alpha)-CH_2(\beta)-$ protons of amino acidate. P. I. Vestues and R. B. Martin, *J. Am. Chem. Soc.*, **102**, 7906 (1980); U. Sakaguchi and H. Yoneda, *Chem. Lett.*, **1976**, 613.